A Packaged Self-Powered System with Universal Connectors Based on Hybridized Nanogenerators

Bojing Shi, Qiang Zheng, Wen Jiang, Ling Yan, Xinxin Wang, Hong Liu, Yan Yao, Zhou Li, and Zhong Lin Wang**

Implantable medical devices, integrated wireless healthcare sensors, and portable electronics are attracting extensive attention,[1] but the batteries used for powering these devices usually display a limited lifetime.[2] Although battery technology has improved, sustainable power sources for cardiac pacemakers, neural stimulators, and other implantable biomedical devices are required. Mechanical energy was considered as one of most abundant and accessible energy sources around the human body.[3] When a small system can efficiently convert mechanical energy in our daily life, this system would be a suitable solution for electricity generation and significantly extend the lifetime of the electronic devices.[4]

Piezoelectric material is one of appropriate choices to fabricate mechanical-to-electrical energy transduction devices.[5] Some of these piezoelectric energy harvesters are made of biocompatible materials possible for in vivo applications, and great progress has been made in this field;[6] Meanwhile, the relatively low outputs limit the application of piezoelectric devices for powering implantable medical devices. Recently, triboelectric nanogenerators (TENGs) have attracted much attention and been considered as another potential solution for harvesting mechanical energy.[7] With their high output performance, outstanding biocompatibility, and low cost, TENGs have been studied for powering implantable medical devices and portable electronics.[8] However, before using these above-mentioned energy transduction devices to power implantable and portable electronic devices, there are still some crucial problems that need to be addressed. For example, the output of implantable triboelectric nanogenerators (iTENGs) needs to be enhanced for further application. Encapsulation is also an essential part of the implantable devices for protecting them from the contamination or liquid infiltration of the surrounding environment. Another important consideration is the versatility of the energy harvesters, which can facilitate the integration of the iTENG and various implantable medical electronics and promote the development of self-powered implantable medical devices and wearable/portable electronics.

Here, we present a piezoelectric and triboelectric hybrid nanogenerator (PTNG) for enhanced output and a packaged self-powered system by hybridizing nanogenerators (PSNGS) based on the PTNG. We also designed viable inner connections and universal outlet connectors for the system. The power management elements and nanogenerator (NG) were integrated on a flexible substrate; therefore, the entire system could be a "Plug and Play" mobile power source. The system was also packaged by poly(dimethylsiloxane) (PDMS) as a waterproof implantable full energy unit for implantable medical devices.

The PTNG was fabricated based on the contact-separation working mode, whereas the contact layer was a $BaTiO_3$@PDMS film. **Figure 1**a showed the structure of the PTNG that was integrated in the PSNGS. When stretched, the polarized $BaTiO_3$@PDMS film will generate piezoelectric potential.[9] This potential can be coupled with the triboelectric effect and increase the output performance of PTNG. A thin Au film (50 nm) was deposited on the $BaTiO_3$@PDMS film as an electrode layer. An aluminum foil modified with nanostructures served as the contact layer and another electrode of the PTNG. A flexible PDMS spacer (500 μm in thickness) was between two contact layers (Figure 1a). To fit the potential in vivo applications, the size of the PTNG was carefully controlled at 1.5 cm × 1.5 cm × 0.2 cm. The contact area was only ≈1.2 cm × 1.2 cm, which subsequently affected the output performance of the PTNG.

The working mechanism of the PTNG is demonstrated in **Figure 2**a. When an external force was applied on the PTNG, the $BaTiO_3$@PDMS film contacted the aluminum foil. Because of the triboelectric effect, electrons were injected from the aluminum foil into the $BaTiO_3$@PDMS film, leaving positive triboelectric charges on the surface of the aluminum foil. Simultaneously, $BaTiO_3$ NPs induced a piezoelectric potential when the $BaTiO_3$@PDMS film was pressed.[10] The positive piezoelectric

B. Shi, Dr. Q. Zheng, W. Jiang, Dr. X. Wang, Prof. H. Liu, Prof. Z. Li, Prof. Z. L. Wang
Beijing Institute of Nanoenergy and Nanosystems
Chinese Academy of Science
Tower C, Techart Plaza
No. 30 Xueyuan Road, Haidian District
Beijing 10083, P. R. China
E-mail: zli@binn.cas.cn; zlwang@binn.cas.cn
L. Yan
Key Laboratory for Biomechanics and Mechanobiology of Ministry of Education
School of Biological Science and Medical Engineering
Beihang University
No. 30 Xueyuan Road, Haidian District
Beijing 10083, P. R. China
Dr. Y. Yao
Department of Cardiology
Beijing Anzhen Hospital
Capital Medical University
Beijing, Institute of Heart Lung and Blood Vessel Diseases
Beijing 100029, P. R. China
Prof. Z. L. Wang
School of Materials Science and Engineering
Georgia Institute of Technology
Atlanta, GA 30332, USA

DOI: 10.1002/adma.201503356

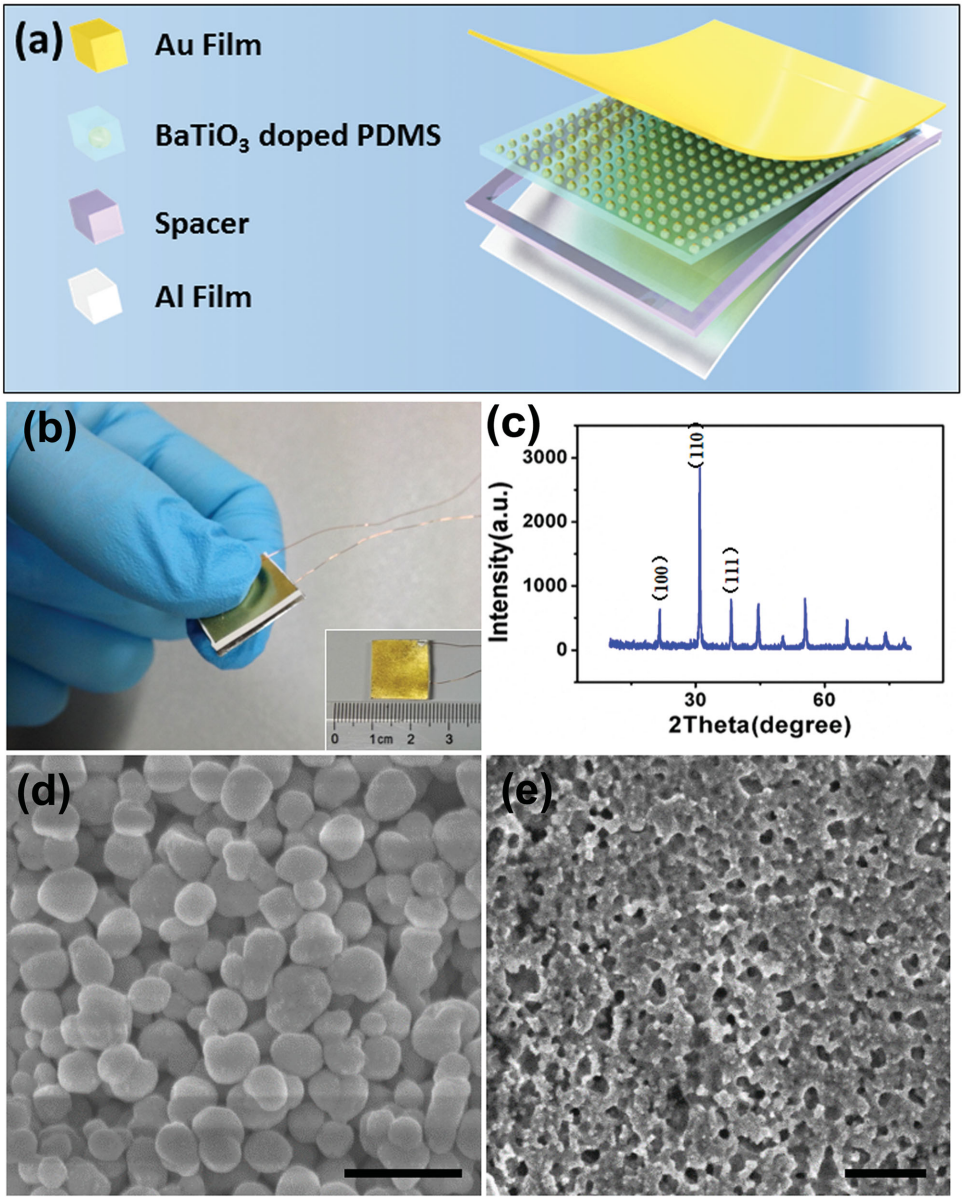

Figure 1. Structural design of the PTNG. a) Schematic diagram of the formation of the PTNG. b) Photograph of the PTNG. c) X-ray diffraction (XRD) pattern of $BaTiO_3$ NPs. d) Scanning electron microscopy (SEM) image of $BaTiO_3$ NPs. The scale bar is 500 nm. e) SEM image of the aluminum film disposed by chemical etching. The scale bar is 500 nm.

potential on the top surface of the $BaTiO_3$@PDMS film could attract more electrons from the aluminum foil. Therefore, the entire positive potential on the aluminum foil was generated by triboelectric charges and the piezoelectric potential of $BaTiO_3$ NPs. With decrease in the external force, the aluminum foil and the $BaTiO_3$@PDMS film were departed with each other. The electric potential difference between the two electrodes caused the electrons to transfer from Au electrode to aluminum foil in the external load. The PTNG then returned to its original state and the positive triboelectric charges on the aluminum foil were completely screened, but negative triboelectric charges remained on the top surface of the $BaTiO_3$@PDMS film. Next, the approach process occurred again. The electrical potential of the Au electrode was higher than that of the aluminum foil resulting in the electrons transfer from the aluminum foil to the Au electrode in the external load. When the $BaTiO_3$@PDMS film was bent and contacted with the aluminum foil, the piezoelectric potential generated and influenced the triboelectric charges again. In this periodic process of contact and separation, electrons were driven back and forth between the two electrodes. The explanation of the electric energy generation process of the PTNG referred to the work about the triboelectric nanogenerator.[11]

To quantitatively analyze the output of the as fabricated PTNG, a liner motor was applied to provide the mechanical motion. As driven by the liner motor at a frequency of 1 Hz, the open circuit voltage (V_{oc}) and the short circuit current (I_{sc})

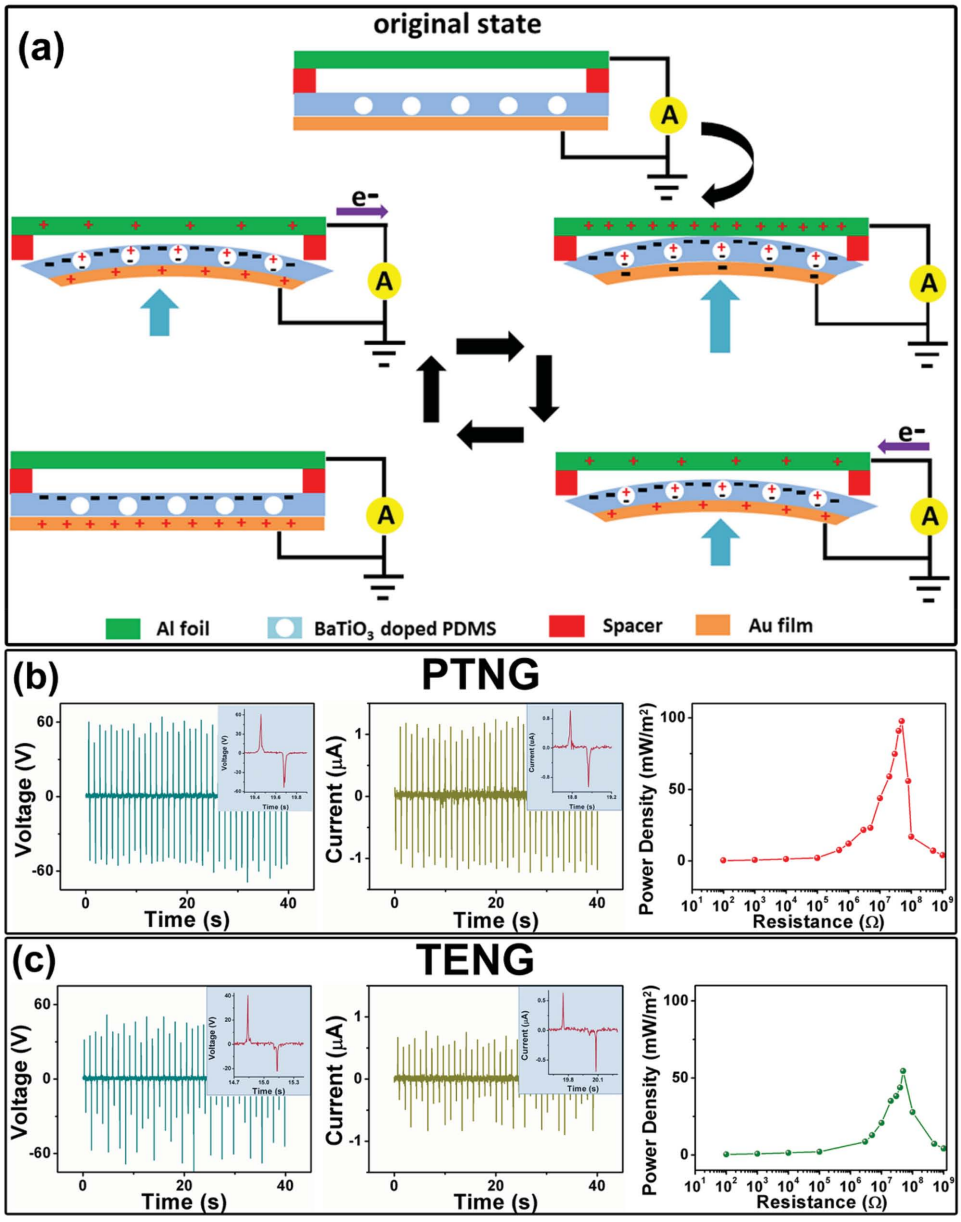

Figure 2. a) A cycle of the electricity generation process describing the working mechanism of the PTNG. b) The open-circuit voltage, short-circuit current, and output power density of the PTNG. c) The open-circuit voltage, short-circuit current, and output power density of the TENG.

of the PTNG and TENG were measured. Typically, the average amplitude of the V_{oc} and the I_{sc} of TENG in the size were 40 V and 0.5 μA, respectively (Figure 2). The V_{oc} and the I_{sc} of PTNG could be increased to 60 V and 1 μA, respectively. With an external load of 50 MΩ applied, the power density could reach 97.41 mW m^{-2} (Figure 2d), which was increased by 80%.

As shown in **Figure 3**a, the PSNGS mainly consist of four parts: the power source (PTNG), a rectifier, a microbattery, and a flexible substrate. When considering the further implantable or portable applications, the size of the PSNGS should be strictly controlled. We tested the electrical properties of the power supply unit. Under the periodic motion of the liner motor, the voltage of the microbattery (EnerChip CBC012; Cymbet Corporation) was charged by the PTNG from 0.5 to 3 V within 30 000 cycles (Figure 3c). The capacity of the battery was 0.108 J. When we increase the motion frequency of the liner motor, the charging time will be shorter. Because of the impedance mismatch between the PTNG and the energy storage part (including the reflector and the battery), the load voltage was lower than the open-circuit voltage of PTNG. We can lower the output voltage and increase the output current like Tang et al. proposed[12] for decreasing the energy-loss ratio of PSNGS.

For future applications of the nanogenerator, miniaturization and low power consumption of the connectors should be considered. The universal sockets and plugs should have low power loss, high durability, and a high ability to prevent short

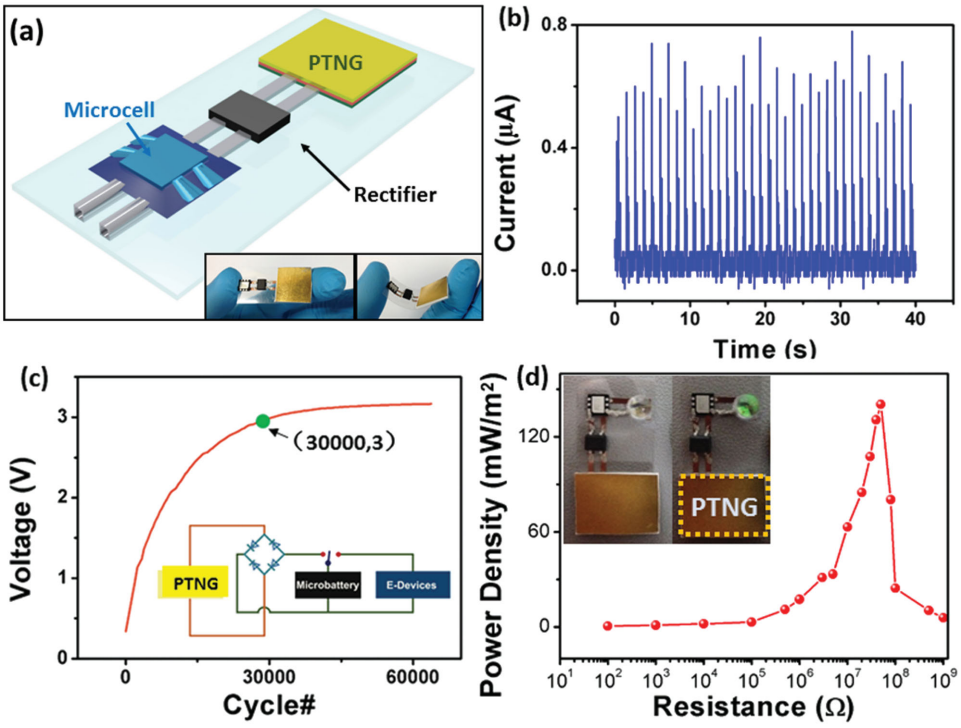

Figure 3. a) Schematic diagram and photograph of the PSNGS. b) Rectified current of the PTNG. c) The charging curve of the microbattery charged by the PTNG. d) The power density of the PTNG. The inset photograph is the integrated PSNGS and a LED.

circuits between devices. Furthermore, a nanogenerator can be used as an electric sensor for multiple signals. With signal transmission, the universal sockets and plugs will expand the potential application of the PSNGS. For example, the universal sockets and plugs can be used to transmit electricity and signals. An implantable PSNGS next to the human heart can detect and evaluate cardiac function by recognizing motion through the PTNG. The PSNGS can also provide the power required to drive medical devices to cure arrhythmia.

To enable the PSNGS to be used as a "Plug and Play" power source for implantable and portable electronics, we designed several universal sockets and plugs that can be integrated with the PSNGS (**Figure 4**). We also used these designed universal sockets and plugs to connect the PSNGS with select low power consumption devices directly. The power and signal transmission are the key features of sockets and plugs. The signal transmission line is illustrated in Figure S3 (Supporting Information).

The first design was a "PIN"-type connector as shown in **Figure** 4a and **5**a. This connector was composed of two parts: the socket consisted of two small hollow cylinders comprised of aluminum foil and the plug part consisted of two adaptable copper wires. After being charged by the PTNG, the PSNGS were connected with four commercial light-emitting-diode (LED) segment displays by "PIN"-type connectors and successfully powered the LED to display "bin." We also used an electronic thermometer to demonstrate the connection between medical devices and the PSNGS. After plugging the electronic thermometer with the PSNGS by a "PIN"-type connector, a finger temperature was measured and shown on the screen.

For the potential application of PSNGS in implantable and waterproof wearable electric devices, we packaged the PSNGS and the universal socket by PDMS (the thickness is 560 μm). Figure 4c,d showed that after placing the packaged PSNGS into normal saline after 12 h, the device can still work by connecting the LED segment displays with the PSNGS through the "PIN"-type connector. After packaging, the PSNGS and the universal socket showed significant stability, waterproof, and hermetical properties for the power supply unit. The process of PTNG working and charging battery in water was shown in Video S1 and S2 (Supporting Information).

In addition, we also used the universal micro-USB as the connector of the PSNGS as shown in Figure 4 and 5. After connecting electronic thermometer with PSNGS, the temperature sensor was placed into the incision to detect the subcutaneous temperature of a live rat. A self-powered "Plug and Play" power unit may play an important role in emergency cases; for example, by harvesting and storing the energy from human motion, this power supply unit can provide energy to portable electronics such as defibrillators or pacemakers.

We tested the energy loss ratio of the connectors between the PSNGS and electronic device (Figure S1, Supporting Information). The results (Figure S2a,b, Supporting Information) showed that for voltages below 2 V, the energy loss ratio of the "PIN"-type and the "USB"-type connector were ≈0.6–1.6% and 0.15–0.48%, respectively. This result indicated that both connectors presented a low energy loss ratio for transferring electric energy between PSNGS and device.

The striking features of the "PIN"-type connector were flexible, inexpensive, and easily packaged. Furthermore, this type

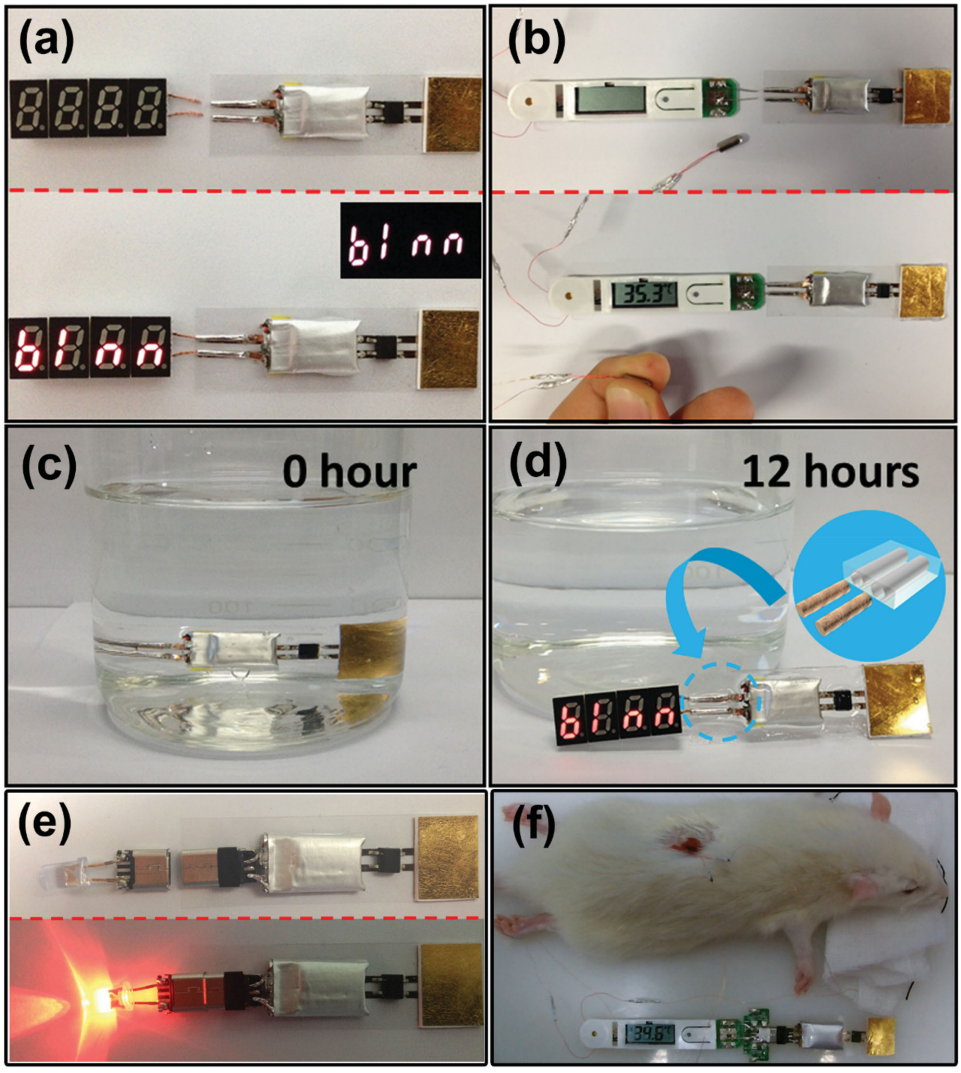

Figure 4. a) Photograph of the "Plug and Play" PSNGS driving four commercial LED segment displays. b) Photograph of the "Plug and Play" PSNGS driving a commercial thermometer. c,d) Photograph of the PSNGS submerged into normal saline showing that 12 h later, the PSNGS can still operate normally. e) The PSNGS with a micro-USB connector can drive the LED light. f) The PSNGS with a micro-USB connector used for a body temperature transducer implanted in a rat.

of connector can be manufactured in small sizes, a key factor for miniaturizing PSNGS. The advantage of a micro-USB connector was a stable and high-speed signal transduction in addition to the low-loss power transmission. However, a micro-USB connector was difficult to be packaged and be applied in flexible electronics. When the micro-USB connector was bent, the connection and stability were destroyed. The package also lost the waterproof and hermetically sealed properties in our test.

Comparing these two types of connectors, we designed a new universal socket and plug combining the advantages of the individual connectors (Figure 5c). This new connector, called an ICP (implantable connector for PSNGS), is composed of three main components: a plug, a socket, and a cavity. The structure of the plug was formed by metal electrodes and insulators configured similar to a coaxial cable. The core was a metal wire (the gray part in Figure 5c) composed of titanium or stainless steel which are adapted for in vivo applications. The core metal wire can be used as the main energy and signal transmission electrode. A thin shell layer outside the metal core (the green part) was a polymer (such as poly(tetrafluoroethylene) (PTFE)) to protect and isolate the core electrode. Several metal ribbons were added on the insulator as additional electrodes for energy and signal transmission. The main and additional electrode of ICP can work separately and synergistically. An entire shell (the blue part) was coated at the outside of the plug as an entire insulator. The socket part was complementary of the plug. A hollow electrode and several ribbon electrodes corresponded to the core and ribbon electrodes of the plug. The hollow and ribbon electrodes were separated by insulating materials (the purple part) in the ICP.

When considering in vivo applications, a waterproof design was indispensable. We designed two types of structures in the ICP for sealing. Several design inspirations originated from the connector of an implanted pacemaker and pacing lead. First, the metal core and cavity covered by polymers produced

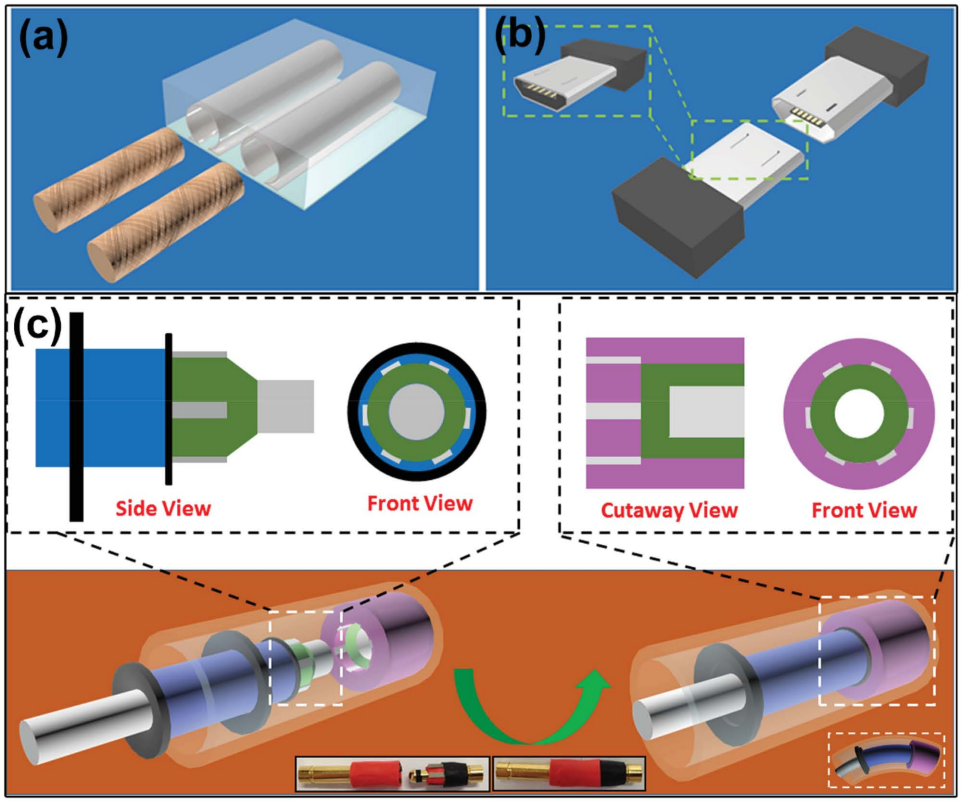

Figure 5. a) Schematic diagram of the "PIN"-type connector for the PSNGS. b) Schematic diagram of the micro-USB connector for the PSNGS. c) Schematic diagram of the next generation connector ICP for the PSNGS. The inset figures are the brief physical maps of the design of the ICP.

a connector such as a piston, which was good for a hermetical seal. Second, two rubber rings (the black part) were designed at the central part and tail of the plug. These two rubber rings constituted a sealing structure that can hold air between them and prevent water seepage. This double protection produced a more reliably waterproof ICP. We fabricated a connector for demonstration in Figure 5c. According to the structure and energy loss of the "PIN"-type and micro-USB connector, the ICP might display a lower energy loss, better waterproof and better signal transmission properties. Furthermore, the ICP can be fabricated to be flexible (Figure 5c) by selecting appropriate materials such as a conductive polymer. The ICP was also primarily designed of PSNGS and provides a reference for PSNGS applied in implanted medical devices, wearable smart portable electronics and microself-powered devices in the future.

In summary, we fabricated a PSNGS based on a PTNG. This hybrid nanogenerator can improve the output and generate up to 60 V and 1 μA with 1.5 cm × 1.5 cm × 0.2 cm in size, respectively. We also designed viable inner connections and universal outlet connectors for the system. The power management elements and the PTNG were integrated on a flexible substrate. This self-powered integrated nanoenergy system was also packaged using biocompatible polymers PDMS to produce a waterproof and implantable PSNGS. We demonstrated the potential of a PSNGS for powering personal and medical electronics as a portable "Plug and Play" power source. This PSNGS will significantly advance the application of the PTNG for waterproof external portable electronics, wearable electronic equipment and in vivo applications of implanted medical devices. Furthermore, connectors were one of the key factors for the application of PSNGS. Therefore, we discussed the design of different connectors between PSNGS and electronic devices, which may establish a standard because of waterproof, fine signal transmission, and flexible properties. Our design of universal connectors can provide a reference for researchers to develop self-powered electronics using the PSNGS.

Experimental Section

Fabrication of the $BaTiO_3$@PDMS Film: A 6 mm-thick acrylic sheet was sculptured into a 15 mm × 15 mm × 1 mm groove by precision laser cutting. The $BaTiO_3$ nanoparticles (NPs) (purchased from Aladdin without further purification) were added into the PDMS elastomer (Sylgard 184, Dow corning), of which the composition of $BaTiO_3$ NPs was 10 wt%. The mixture was then stirred for ≈6 h with a mechanical agitator. The well-mixed mixture was then poured into the acrylic groove and cured at 80 °C for 1 h in an oven. A Cr and Au layer was deposited onto the surface of the $BaTiO_3$ film (thickness: 1 mm) by radio frequency magnetron sputtering. Two copper wires were connected to the Au electrode by silver paste, and the $BaTiO_3$ device was then poled at 100 °C by applying an electric field of 20 kV cm^{-1} for 10 h.

Fabrication of Integrated Flexible Circuits: A 2 mm-thick acrylic sheet was cut into a mask using a laser. The mask was then covered on a poly(ethylene terephthalate) (PET) substrate, and the Cu electrode was deposited on the PET substrate by radio frequency magnetron sputtering for 10 min. The width of the Cu electrode was 2 mm and the thickness of the PET substrate was 80 μm. A rectifier and a battery were fastened on

the PET substrate. Finally, silver paste was used to connect the electronic devices and Cu electrode. The NG was then packaged by PDMS.

Electrical Measurement of the PTNG: The PTNG was pressed periodically by a linear motor at a frequency of 1 Hz. The output performance of the PTNG was measured by an oscilloscope and Stanford Research Systems. A Tektronix DPO3034 oscilloscope and SR570 low noise current amplifier were used to detect the voltage and current of PTNG, respectively. The PTNG was then connected with different loads from 100 Ω to 1 GΩ; the load voltages and current were then detected, and the output power of the PTNG was calculated.

Waterproof Test of the PSNGS: The PSNGS was placed into 200 mL of saline (0.9 wt% NaCl solution) and removed after 12 h of submersion at room temperature. After drying naturally, the PSNGS was used to drive commercial LED segment displays of "bin."

The packaged PTNG was put into the water and pressed periodically. The output was shown on the oscilloscope (Video S1, Supporting Information). We also connected PTNG, rectifier, microbattery on a PET substrate and packaged the whole device. The multimeter was used to display the charging of the battery when PTNG was pressed periodically in water (Video S2, Supporting Information).

Animal Tests of Implantable Device Powered by the PSNGS: Adult rats (Hsd: Sprague Dawley SD, male, 100–150 g) used for the experiment were purchased from Peking University Health Science Center (PEUHSC), and our procedures in handling the animals were supervised by the Experimental Animal Ethics Committee of PEUHSC, which strictly followed the "Beijing Administration Rule of Laboratory Animals," and the national standards "Laboratory Animal Requirements of Environment and Housing Facilities (GB 14925-2001)." The rats were narcotized by isoflurane gas and an incision was then made on its back. The electronic thermometer powered by PSNGS was placed under the skin of the rat and detected the temperature of the rat.

Supporting Information

Supporting Information is available from the Wiley Online Library or from the author.

Acknowledgements

B.S. and Q.Z. contributed equally to this work. This work was supported by the "Thousands Talents" program for pioneer researcher and his innovation team, NSFC 31200702, 31571006, Beijing Nova Program Z121103002512019.

Received: July 12, 2015
Revised: September 11, 2015
Published online: December 4, 2015

[1] a) J. A. Rogers, *Nature* **2010**, *468*, 177; b) M. L. Hammock, A. Chortos, B. C. K. Tee, J. B. H. Tok, Z. A. Bao, *Adv. Mater.* **2013**, *25*, 5997; c) B. D. Gates, *Science* **2009**, *323*, 1566; d) C. P. Lau, C. W. Siu, H. F. Tse, *Circulation* **2014**, *129*, 811.

[2] a) C. Algora, R. Pena, *Artif. Organs* **2009**, *33*, 855; b) L. Fang, B. Liang, G. Yang, Y. C. Hu, Q. Zhu, X. S. Ye, *Biosens. Bioelectron.* **2014**, *56*, 91; c) L. C. Rome, L. Flynn, E. M. Goldman, T. D. Yoo, *Science* **2005**, *309*, 1725.

[3] a) S. Wang, Y. Xie, S. Niu, L. Lin, Z. L. Wang, *Adv. Mater.* **2014**, *26*, 2818; b) Y. Yang, H. L. Zhang, Z. H. Lin, Y. S. Zhou, Q. S. Jing, Y. J. Su, J. Yang, J. Chen, C. G. Hu, Z. L. Wang, *ACS Nano* **2013**, *7*, 9213; c) J. H. Lee, K. Y. Lee, M. K. Gupta, T. Y. Kim, D. Y. Lee, J. Oh, C. Ryu, W. J. Yoo, C. Y. Kang, S. J. Yoon, J. B. Yoo, S. W. Kim, *Adv. Mater.* **2014**, *26*, 765; d) J. A. Paradiso, T. Starner, *IEEE Pervas. Comput.* **2005**, *4*, 18.

[4] a) J. Zhong, Y. Zhang, Q. Zhong, Q. Hu, B. Hu, Z. L. Wang, J. Zhou, *ACS Nano* **2014**, *8*, 6273; b) K. C. Pradel, W. Wu, Y. Ding, Z. L. Wang, *Nano Lett.* **2014**, *14*, 6897; c) R. A. Whiter, V. Narayan, S. Kar-Narayan, *Adv. Energy Mater.* **2014**, *4*, 1400519; d) S. P. Beeby, M. J. Tudor, N. M. White, *Meas. Sci. Technol.* **2006**, *17*, R175; e) E. W. Ballentine, S. E. Wahlstrom, *US Patent 3086131*, **1961**, *US Patent 4126822*, **1977**.

[5] a) J. H. Koo, J. Seo, T. Lee, *Thin Solid Films* **2012**, *524*, 1; b) Z. L. Wang, J. Song, *Science* **2006**, *312*, 242; c) Y. Qi, J. Kim, T. D. Nguyen, B. Lisko, P. K. Purohit, M. C. McAlpine, *Nano Lett.* **2011**, *11*, 1331.

[6] a) G. Zhu, A. C. Wang, Y. Liu, Y. Zhou, Z. L. Wang, *Nano Lett.* **2012**, *12*, 3086; b) C. Dagdeviren, B. D. Yang, Y. Su, P. L. Tran, P. Joe, E. Anderson, J. Xia, V. Doraiswamy, B. Dehdashti, X. Feng, B. Lu, R. Poston, Z. Khalpey, R. Ghaffari, Y. Huang, M. J. Slepian, J. A. Rogers, *Proc. Natl. Acad. Sci. USA* **2014**, *111*, 1927; c) H. Zhang, X. S. Zhang, X. L. Cheng, Y. Liu, M. D. Han, X. Xue, S. F. Wang, F. Yang, A. S. Smitha, H. X. Zhang, Z. Y. Xu, *Nano Energy* **2015**, *12*, 296; d) Z. Li, G. Zhu, R. Yang, A. C. Wang, Z. L. Wang, *Adv. Mater.* **2010**, *22*, 2534.

[7] a) F. R. Fan, Z. Q. Tian, Z. L. Wang, *Nano Energy* **2012**, *1*, 328; b) Z. L. Wang, J. Chen, L. Lin, *Energy Environ. Sci.* **2015**, *8*, 2250.

[8] Q. Zheng, B. Shi, F. Fan, X. Wang, L. Yan, W. Yuan, S. Wang, H. Liu, Z. Li, Z. L. Wang, *Adv. Mater.* **2014**, *26*, 5851.

[9] D. R. Chen, X. L. Jiao, *J. Am. Ceram. Soc.* **2000**, *83*, 2637.

[10] K. I. Park, M. Lee, Y. Liu, S. Moon, G. T. Hwang, G. Zhu, J. E. Kim, S. O. Kim, D. K. Kim, Z. L. Wang, K. J. Lee, *Adv. Mater.* **2012**, *24*, 2999.

[11] G. Zhu, Z. H. Lin, Q. S. Jing, P. Bai, C. F. Pan, Y. Yang, Y. S. Zhou, Z. L. Wang, *Nano Lett.* **2013**, *13*, 847.

[12] W. Tang, T. Zhou, C. Zhang, F. R. Fan, C. B. Han, Z. L. Wang, *Nanotechnology* **2014**, *25*, 225402.